



Optoelectronically Optimized Colored Thin-Film Solar Cells

Ahmad, Faiz; Anderson, Tom H.; Lenau, Torben; Lakhtakia, Akhlesh

Published in:
Proceedings of SPIE

Link to article, DOI:
[10.1117/12.2534592](https://doi.org/10.1117/12.2534592)

Publication date:
2019

Document Version
Publisher's PDF, also known as Version of record

[Link back to DTU Orbit](#)

Citation (APA):

Ahmad, F., Anderson, T. H., Lenau, T., & Lakhtakia, A. (2019). Optoelectronically Optimized Colored Thin-Film Solar Cells. In P. Banerjee, K. Gudmundsson, A. Lakhtakia, & G. Subramany (Eds.), *Proceedings of SPIE* (Vol. 11371). [1137107] SPIE - International Society for Optical Engineering. <https://doi.org/10.1117/12.2534592>

General rights

Copyright and moral rights for the publications made accessible in the public portal are retained by the authors and/or other copyright owners and it is a condition of accessing publications that users recognise and abide by the legal requirements associated with these rights.

- Users may download and print one copy of any publication from the public portal for the purpose of private study or research.
- You may not further distribute the material or use it for any profit-making activity or commercial gain
- You may freely distribute the URL identifying the publication in the public portal

If you believe that this document breaches copyright please contact us providing details, and we will remove access to the work immediately and investigate your claim.

PROCEEDINGS OF SPIE

SPIDigitalLibrary.org/conference-proceedings-of-spie

Optoelectronically optimized colored thin-film CZTSSe solar cells

Ahmad, Faiz, Anderson, Tom, Lenau, Torben, Lakhtakia, Akhlesh

Faiz Ahmad, Tom H. Anderson, Torben Lenau, Akhlesh Lakhtakia, "Optoelectronically optimized colored thin-film CZTSSe solar cells," Proc. SPIE 11371, International Workshop on Thin Films for Electronics, Electro-Optics, Energy, and Sensors 2019, 1137107 (6 December 2019); doi: 10.1117/12.2534592

SPIE.

Event: International Workshop on Thin Films for Electronics, Electro-Optics, Energy and Sensors, 2019, Reykjavik, Iceland

Optoelectronically optimized colored thin-film CZTSSe solar cells

Faiz Ahmad^a, Tom H. Anderson^b, Torben Lenau^c, and Akhlesh Lakhtakia^a

^aPennsylvania State University, Department of Engineering Science and Mechanics,
University Park, PA 16802, USA

^bUniversity of Delaware, Department of Mathematical Sciences, Newark, DE 19716, USA

^cTechnical University of Denmark, Department of Mechanical Engineering,
DK-2800 Lyngby, Denmark

ABSTRACT

Rooftop solar cells may become more acceptable if they are colored, e.g., red or blue-green, which requires that a certain part of the incoming solar spectrum be reflected. We implemented and optimized an optoelectronic model for $\text{Cu}_2\text{ZnSn}(\text{S}_\xi\text{Se}_{1-\xi})_4$ (CZTSSe) solar cells containing (i) a conventional 2200-nm-thick CZTSSe layer with homogeneous bandgap, or (ii) an ultrathin CZTSSe layer with optoelectronically optimized sinusoidally nonhomogeneous bandgap, or (iii) a CZTSSe layer with optoelectronically optimized linearly nonhomogeneous bandgap. Either complete or partial rejection of either red or blue-green photons was incorporated in the model. Calculations show that on average, the efficiency of a typical solar cell will be reduced by about 9% if 50% red photons are reflected or by about 13% if 50% blue-green photons are reflected. The efficiency reduction increases to about 18% if all red photons are reflected or about 26% if all blue-green photons are reflected.

Keywords: colored solar cell, CZTSSe, optoelectronic optimization, thin-film solar cell

1. INTRODUCTION

Photovoltaic solar cells represent an eco-friendly source of energy. However, they take up valuable land that otherwise could be used for other purposes such as farming. Rooftops are promising alternatives since they have the only function. But, many homeowners and their tenants appreciate the aesthetic appearance of their living and working spaces, and some of them resist the installation of solar panels on rooftops due to visual change.¹ Solar cells are typically bluish black and have macroscopically uniform flat surfaces, those features providing the maximum energy output. Roof claddings, such as red clay tiles, are often colored and have corrugated surfaces, in contrast. The aesthetic requirements can be met by coloring solar cells either red or blue-green.

Red or blue-green rejection filters can be made of particulate composite materials containing, say, silica nanospheres. Typically, the solar cells will be iridescent then, which may not be aesthetically pleasing to many. Non-iridescent colored rejection filters can be fabricated by properly scaling the linear dimensions of biomimetic filters nano-imprinted to reproduce the *Morpho* blue,² this possibility being guaranteed by the scale invariance of the Maxwell equations and the weak dispersion of the refractive indexes of numerous polymers in the visible spectral regime.

Further author information: (Send correspondence to Faiz Ahmad)

Faiz Ahmad: E-mail: fua26@psu.edu

2. OPTOELECTRONIC MODEL

Computational modeling of photovoltaic cells can determine the efficiency loss to achieve the desired color by the rejection of photons in a specific spectral regime. Hence, we implemented and optimized a thin-film $\text{Cu}_2\text{ZnSn}(\text{S}_\xi\text{Se}_{1-\xi})_4$ (commonly referred to as CZTSSe) solar cell for two different desired colors: (i) red and (ii) blue-green. Accordingly, either the red part (620-700 nm wavelength) or the bluish-green part (400-550 nm wavelength) of the incoming solar spectrum must be substantially reflected so that it becomes mostly unavailable for the photovoltaic generation of electricity. Therefore, we used an optoelectronic model of CZTSSe solar cells³ to optimize them for maximum power conversion efficiency while reflecting either red photons or blue-green photons.

A conventional CZTSSe solar cell has the $\text{MgF}_2/\text{AZO}/\text{iZnO}/\text{CdS}/\text{CZTSSe}/\text{Mo}(\text{S},\text{Se})_2/\text{Mo}$ configuration, beginning with a MgF_2 layer of thickness L_{MgF_2} as the antireflection coating; an AZO layer of thickness L_{AZO} as the front contact; an iZnO layer and a CdS layer of thicknesses L_{iZnO} and L_{CdS} , respectively, forming a buffer; a CZTSSe layer of thickness L_s as the photovoltaic layer; an $\text{Mo}(\text{S},\text{Se})_2$ layer formed as a consequence of the deposition process; and a Mo back-contact/backreflector of thickness L_m . The formation of the $\text{Mo}(\text{S},\text{Se})_2$ layer deleteriously affects the solar-cell performance by adding a series resistance and increasing the back-surface electron-hole pair recombination rate. To avoid the formation of the $\text{Mo}(\text{S},\text{Se})_2$ layer, the introduction of a thin Al_2O_3 passivation layer (of thickness L_a) between the Mo back-contact/backreflector and the CZTSSe photovoltaic layer has been proposed,⁴ and we incorporated this suggestion in our model; see Fig. 1. Also, we replaced the conventional flat back-contact/backreflector with a 1D periodically corrugated one for better light trapping.^{5,6} The period, duty cycle, and height of the periodically corrugated backreflector are denoted by L_x , $\zeta \in (0, 1)$, and L_g , respectively.

The nonhomogeneous bandgap in the CZTSSe layer was taken to be either sinusoidally or linearly graded.³ Linearly graded bandgaps of two types were considered: (a) forward graded and (b) backward graded. The linear backward bandgap grading was modeled as

$$\begin{aligned} E_g(z) &= E_{g,\max} - A(E_{g,\max} - E_{g,\min}) \frac{z - (L_{\text{MgF}_2} + L_{\text{AZO}} + L_{\text{iZnO}} + L_{\text{CdS}})}{L_s}, \\ z &\in [L_{\text{MgF}_2} + L_{\text{AZO}} + L_{\text{iZnO}} + L_{\text{CdS}}, L_{\text{MgF}_2} + L_{\text{AZO}} + L_{\text{iZnO}} + L_{\text{CdS}} + L_s], \end{aligned} \quad (1)$$

where $E_{g,\min}$ is the minimum bandgap, $E_{g,\max}$ is the maximum bandgap, and A is an amplitude (with $A = 0$ representing a homogeneous CZTSSe layer). The linear forward bandgap grading was modeled by

$$\begin{aligned} E_g(z) &= E_{g,\min} + A(E_{g,\max} - E_{g,\min}) \frac{z - (L_{\text{MgF}_2} + L_{\text{AZO}} + L_{\text{iZnO}} + L_{\text{CdS}})}{L_s}, \\ z &\in [L_{\text{MgF}_2} + L_{\text{AZO}} + L_{\text{iZnO}} + L_{\text{CdS}}, L_{\text{MgF}_2} + L_{\text{AZO}} + L_{\text{iZnO}} + L_{\text{CdS}} + L_s]. \end{aligned} \quad (2)$$

The sinusoidal bandgap grading was modeled as

$$\begin{aligned} E_g(z) &= E_{g,\min} + A(1.49 - E_{g,\min}) \times \left\{ \frac{1}{2} \left[\sin \left(2\pi K \frac{z - (L_{\text{MgF}_2} + L_{\text{AZO}} + L_{\text{iZnO}} + L_{\text{CdS}})}{L_s} - 2\pi\psi \right) + 1 \right] \right\}^\alpha, \\ z &\in [L_{\text{MgF}_2} + L_{\text{AZO}} + L_{\text{iZnO}} + L_{\text{CdS}}, L_{\text{MgF}_2} + L_{\text{AZO}} + L_{\text{iZnO}} + L_{\text{CdS}} + L_s], \end{aligned} \quad (3)$$

where $\psi \in [0, 1]$ describes a relative phase shift, K is the number of periods in the CZTSSe layer, and $\alpha > 0$ is a shaping parameter.

The optoelectronic model was used to determine the effects of the rejection filter on the short-circuit density, the open-circuit voltage, the efficiency, and the fill factor. These parameters were calculated for normally incident unpolarized solar radiation using the rigorous-coupled wave approach for the photon absorption rate and, therefore, the electron-hole-pair generation rate. The transport of electrons and holes in the iZnO/CdS/CZTSSe region was considered using the 1D drift-diffusion model with the assumption of ideal ohmic front and back-contact. A hybridizable discontinuous Galerkin scheme^{7,8} was used for the drift-diffusion equations. Band-gap varying electron affinity and defect density of states were incorporated in the model, as also were the Shockley-Read-Hall and radiative electron-hole recombination processes.⁹ The differential evolution algorithm¹⁰ was used to optimize the efficiency for (i) no rejection ($f = 0$), (ii) 50% rejection ($f = 0.5$), and (iii) 100% rejection ($f = 1.0$) of either red or blue-green photons.

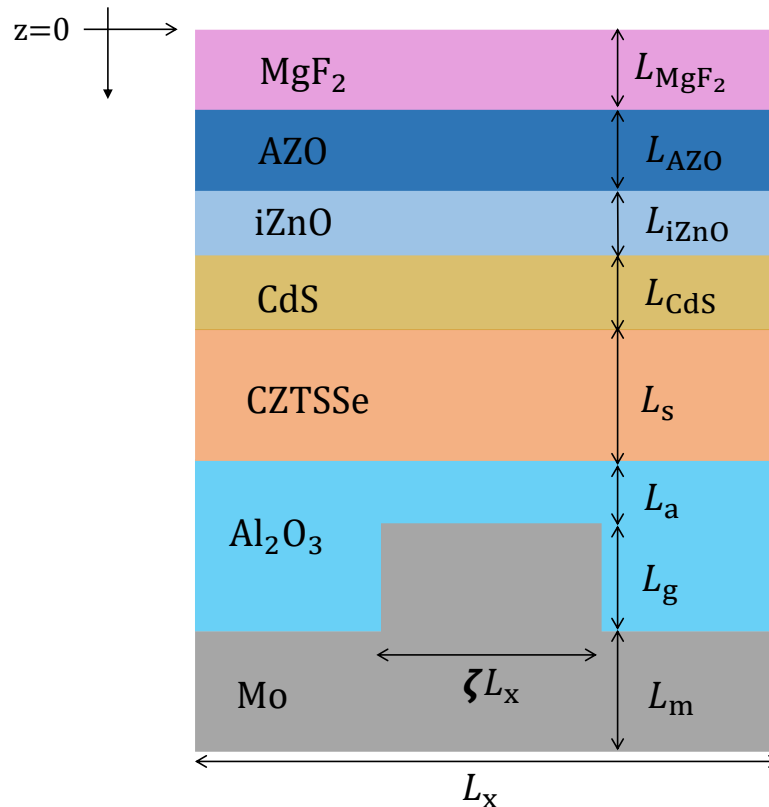


Figure 1. Schematic of the reference unit cell of the CZTSSe solar cell with a 1D periodically corrugated metallic backreflector of period L_x and duty cycle $\zeta \in (0, 1)$.

3. NUMERICAL RESULTS AND CONCLUSION

First, we considered the CZTSSe layer to have a homogeneous bandgap and the metallic back reflector 1D periodically corrugated backreflector. Values of the short-circuit current density J_{sc} , open-circuit voltage V_{oc} , efficiency η , and fill factor FF are shown in Table 1 with $f \in \{0, 0.5, 1.0\}$ of either red or blue-green photons. Also, the percentage relative reduction in efficiency with respect to no rejection ($f = 0$) is provided in the same table. For a conventional 2200-nm-thick CZTSSe solar cell with a 1D periodically corrugated backreflector, the optoelectronic model predicts the optimal solar cell's efficiency without any rejection filter to be 11.8%. The optimal efficiency reduces to 10.7% if 50% red photons are rejected and 9.6% with 100% rejection of red photons. The optimal efficiency reduces to 10.2% and 8.7% with 50% and 100% rejection of blue-green photons, respectively.

Next, we considered optimization of linearly nonhomogeneous bandgap solar cells according to Eqs. (1) and (2). The optimal CZTSSe solar cell with a backward linearly nonhomogeneous bandgap [Eq. (1)] was found to be the same as the 2200-nm-thick conventional homogeneous solar cell. For the forward linearly nonhomogeneous bandgap [Eq. (1)], the optimization predicted $A \neq 0$. Values of J_{sc} , V_{oc} , η , FF and % η reduction are shown in Table 1. For the forward linearly nonhomogeneous bandgap, the efficiency without any rejection filter is 17.0% with a 2200-nm-thick CZTSSe absorber layer. The efficiency reduces to 15.91% with 50% and 14.3% with 100% rejection of red photons. The efficiency reduces to 15.2% and 13.4% with 50% and with 100% rejection of blue-green photons, respectively.

Finally, we considered the sinusoidally nonhomogeneous bandgap described by Eq (3). Values of J_{sc} , V_{oc} , η , FF and % reduction in η are shown in Table 1. The efficiency without any photon rejection is 21.74% with an

Table 1. Values of J_{sc} , V_{oc} , η , FF and % reduction in η relative to $f = 0$ of the optimal CZTSSe solar cell when the CZTSSe layer is either homogeneous or linearly graded according to Eq. (2) or sinusoidally graded according to Eq. (3) and periodically corrugated backreflector. Here, $f \in \{0, 0.5, 1\}$ denotes the fraction of either red or blue-green photons that could have been absorbed but were rejected by the incorporation of a rejection filter.

Cell type	Thickness (nm)	Reflected color	f	J_{sc} (mA cm ⁻²)	V_{oc} (V)	FF (%)	η (%)	% reduction of η
Homogeneous bandgap	2200		0	31.5	558	70.3	11.8	
		Red	0.5	29.0	536	69.0	10.7	9.3
			1	26.3	532	68.8	9.6	18.6
		Blue-green	0.5	28.0	534	68.6	10.2	13.5
			1	24.3	527	68.0	8.7	26.2
Linearly graded bandgap	2200		0	36.7	628	74.0	17.0	
		Red	0.5	34.8	619	73.7	15.9	6.4
			1	31.8	614	73.1	14.3	15.8
		Blue-green	0.5	33.5	617	73.5	15.2	10.5
			1	30.0	611	72.9	13.4	21.1
Sinusoidally graded bandgap	870		0	37.3	772	75.2	21.7	
		Red	0.5	36.1	770	74.1	20.6	5.0
			1	33.3	767	73.6	18.8	13.3
		Blue-green	0.5	35.2	769	73.8	20.0	7.8
			1	31.5	764	73.3	17.7	18.4

optimal ultrathin 870 nm CZTSSe layer in Table 1. For this solar cell, the efficiency reduces to 20.6% with 50% rejection and 18.8% with 100% rejection of red photons. The efficiency reduces to 20.0% and 17.7% with 50% and 100% rejection of blue-green photons, respectively.

The relative reduction in efficiency is $7.05 \pm 2.05\%$ with 50% rejection and $15.80 \pm 2.70\%$ with 100% rejection of red photons in Table 1. The analogous figures are $10.40 \pm 2.70\%$ and $22.35 \pm 3.85\%$ when blue-green photons are rejected. The main reason for higher efficiency reduction with blue-green rejection filters is that sunlight contains 42% more blue-green photons than red photons. The efficiency reduction is mainly due to reduction in the short-circuit current density; however, the open-circuit voltage and the fill factor are affected very little.

In conclusion, the emergence and commercialization of solar cells with red or blue-green appearance will enhance the adoption of solar cells for rooftop installation. Our optoelectronic modeling predicts that the reduction in efficiency due to the deployment of a color rejection filter can be compensated by the use of a graded-bandgap semiconductor layer and light-trapping techniques.

Acknowledgments. The authors thank Peter B. Monk (University of Delaware) for continued collaboration and guidance. The research of Faiz Ahmad and Akhlesh Lakhtakia was partially supported by US National Science Foundation (NSF) under grant number DMS-1619901. The research of Tom H. Anderson was partially supported by the US NSF under grant number DMS-1619904.

REFERENCES

- [1] Lenau, T., Ahmad, F., and Lakhtakia, A., “Towards biomimetic red solar cells,” *Proceedings of SPIE* **10965**(1), 109650E (2019).
- [2] Saito, A., Murase, J., Yonezawa, M., Watanabe, H., Shibuya, T., Sasaki, M., Ninomiya, T., Noguchi, S., Akai-Kasaya, M., and Kuwahara, Y., “High-throughput reproduction of the Morpho butterfly’s specific high contrast blue,” *Proceedings of SPIE* **8339**(1), 83390C (2012).
- [3] Ahmad, F., Lakhtakia, A., Anderson, T.H., and Monk, P.B., “Towards highly efficient thin-film solar cells with a graded-bandgap CZTSSe layer,” preprint.
- [4] Liu, F., Huang, J., Sun, K., Yan, C., Shen, Y., Park, J., Pu, A., Zhou, F., Liu, X., Stride, J.A., Green, M.A., and Hao, X., “Beyond 8% ultrathin kesterite $\text{Cu}_2\text{ZnSnS}_4$ solar cells by interface reaction route controlling and self-organized nanopattern at the back contact,” *NPG Asia Materials* **9**(1), e401 (2017).
- [5] Faryad, M., and Lakhtakia, A., “Enhancement of light absorption efficiency of amorphous-silicon thin-film tandem solar cell due to multiple surface-plasmon-polariton waves in the near-infrared spectral regime,” *Optical Engineering* **52**(8), 087106 (2013).
- [6] Khaleque, T., and R. Magnusson, R., “Light management through guided- mode resonances in thin-film silicon solar cells,” *Journal of Nanophotonics* **8**(1), 083995 (2014).
- [7] Cockburn, B., Gopalakrishnan, J., and Lazarov, R., “Unified hybridization of discontinuous Galerkin, mixed, and continuous galerkin methods for second order elliptic problems,” *SIAM Journal on Numerical Analysis* **47**(2), 1319–1365 (2009).
- [8] Brinkman, D., Fellner, K., Markowich, P., and Wolfram, M.-T., “A drift-diffusion-reaction model for excitonic photovoltaic bilayers: Asymptotic analysis and a 2-D HDG finite-element scheme,” *Mathematical Models and Methods in Applied Sciences* **23**(5), 839–872 (2013).
- [9] Adachi, S., [Earth-Abundant Materials for Solar Cells: $\text{Cu}_2\text{-II-IV-VI}_4$ Semiconductors], Wiley, Chicester, United Kingdom, 2015.
- [10] Storn, R., and Price, K., “Differential evolution—a simple and efficient heuristic for global optimization over continuous spaces,” *Journal of Global Optimization* **11**(4), 341–359 (1997).